I.J. Image, Graphics and Signal Processing, **2023, 5, 77-87**
Published Online on October 8, 2023 by MECS Press (http://www.mecs-press.org/)
DOI: 10.5815/ijigsp.2023.05.06

Information Technology for Multiparametric Analysis of Laser Images of Biological Fluid Films in Biomedical Applications

Yuriy Ushenko*
Computer Science Department,Yuriy Fedcovitch Chernivtsi National University, Chernivtsi, 58002, Ukraine
E-mail: y.ushenko@chnu.edu.ua*
ORCID ID: https://orcid.org/0000-0003-1767-1882
*Corresponding Author

Ivan Gordey
Computer Science Department,Yuriy Fedcovitch Chernivtsi National University, Chernivtsi, 58002, Ukraine
E-mail: hordei.ivan@chnu.edu.ua
ORCID ID: https://orcid.org/0000-0003-3179-0394

Yuriy Tomka
Computer Science Department,Yuriy Fedcovitch Chernivtsi National University, Chernivtsi, 58002, Ukraine
E-mail: y.tomka@chnu.edu.ua
ORCID ID: https://orcid.org/0000-0002-0495-3090

Irina Soltys
Optics and Publishing Department,Yuriy Fedcovitch Chernivtsi National University, Chernivtsi, 58002, Ukraine
E-mail: i.soltys@chnu.edu.ua
ORCID ID: https://orcid.org/0000-0003-2156-7404

Oksana Bakun
Bucovinian State Medical University, Chernivtsi, 58000, Ukraine
E-mail: kupchanko06@gmail.com
ORCID ID: https://orcid.org/0000-0002-4742-2265

Zhengbing Hu
School of Computer Science, Hubei University of Technology, Wuhan, China
E-mail: drzbhu@gmail.com
ORCID ID: https://orcid.org/0000-0002-6140-3351

Received: 10 February 2023; Revised: 18 April 2023; Accepted: 20 May 2023; Published: 08 October 2023

Abstract: At the current moment, all developed polarization methods utilize "single-point" statistical analysis algorithms for laser fields. A relevant task is to generalize traditional techniques by incorporating new correlation-based "two-point" algorithms for the analysis of polarization images. Theoretical foundations of the mutual and autocorrelation processing of phase maps of polarization-structural images of samples of dehydrated serum films are given. The maps of a new polarization-correlation parameters, namely complex degree of coherence (CDC) and complex degree of mutual polarization (CDMP) of soft matter layer boundary field by the example of dehydrated serum film samples are investigated. Two groups of representative samples, uterine myoma patients (control group 1) and patients with external genital endometriosis (study group 2), were considered. We applied a complex algorithm of analytical data processing - statistical (1stand 4th central statistical moments), correlation (Gram-Charlie expansion coefficients of autocorrelation functions) and fractal (fractal dimensions) parameters of polarization-correlation parameters maps. Objective markers for diagnosing extragenital endometriosis were found.

Index Terms: Laser, Polarization, Blood plasma, Birefringence, Statistics, Correlation, Fractal Analysis.

1. Introduction

Scattering processes of optical radiation by optically inhomogeneous biological objects and media are typically considered in a statistical approach. The main informational parameters in such studies are spatial and temporal changes in intensity, as well as polarization states of electromagnetic waves. This has led to the development of the well-known field of scattering optics - Stokes polarimetry. In parallel, other methods of investigating such structures have emerged, which utilize laser polarized radiation as a probe. The coherence of laser beams necessitated the development of approaches to the analysis of scattered radiation fields that are distinct from statistical methods. Over the last 15-20 years, new directions in the study of scattered polarized coherent radiation have been formed, including fractal optics and singular optics, which employ topological and scale-invariant approaches. Based on these approaches, correlations between sets of statistical moments of the 1st to 4th order, autocorrelation functions, fractal dimensions, characterizing once-scattering optically anisotropic layers of biological tissues, and the polarization parameters of their laser images have been determined. On the other hand, for scattered coherent radiation, the consideration of the degree of correlation between orthogonal components of amplitude becomes crucial. This gives rise to a logical gap between the mechanisms of forming integral (statistical) and local (correlation) polarization characteristics of laser radiation fields transformed by optically anisotropic biological layers.

2. Brief Theory

Among the diverse areas of optical detection of polycrystalline structure of biological objects, a significant place is occupied by the polarization methods [1-6]. Vector-parametric algorithms - matrix operator of object optical field coherence - are the theoretical basis of the mentioned methods [1, 2]. Such matrix operator characterizes the one-point correlation in each point (r) of the objective field of complex amplitude components $E_x(r), E_y(r)$ [3-6]. On their basis, methods of coordinate mapping of polarization structure of boundary field layers of biological tissues (BT) were developed. The results of this analysis made it possible to identify markers of the female reproductive organs of the structure was carried out [7-16].

On the other hand, "single-point" methods of polarimetric imaging and statistical analysis of the obtained data are, to some extent, informationally limited. They do not provide any information about the topographic structure of the polarization images of biological layers, as well as their large-scale self-similarity. Moreover, alongside these methods, correlation and fractal analysis algorithms are practically unused for the objective assessment of such "unexplored" structures in laser images. A new stage in expanding the functional capabilities of traditional polarimetry methods was the correlation generalization of traditional polarimetry methods, called the "two-point" approach. The indicated method uses a correlation analytical approach - determination of the degree of agreement between polarization azimuths and ellipticities at $(r_1, r_1 + \Delta r)$) points of the phase-inhomogeneous optical field [17,18]. Quantitatively, such a correlation was characterized by the value of the modulus of the CDMP correlation parameter $V(r_1, r_1 + \Delta r)$ [19]. A development of this method was using the CDC parameter [20-24], which characterizes the correlation coherence of the polarization manifestations of the optical-anisotropic BT structure and other computer assisted methods [25-27].

As a result, the sensitivity of polarization methods to subtle changes in the polycrystalline structure of biological layers has improved. On this basis the differential diagnosis of different prostate cancer stages has been realized.

A disadvantage of these methods is the need for traumatic and not always safe biopsies of internal organ tissue. Polarization-correlation analysis of object fields of easily accessible biological objects - dehydrated films of human body fluids - may become an alternative to it.

In our study, we explored the possibility of a comprehensive solution to the problem of expanding and clinically utilizing the functional capabilities of digital polarization correlometry in laser imaging of biological fluid films. This was achieved through the following:

- Development of Analytical Jones Matrix Model: We devised an analytical Jones matrix model to describe the formation of polarization-correlation maps in polycrystalline networks of dehydrated films of peritoneal fluid. This model allows us to better understand the polarization properties of the biological sample.
- Application of Algorithmic Complex: We applied a combination of algorithms to evaluate the statistical, correlation, and scale-invariant structures present in polarization-correlation maps. By doing so, we could identify digital criteria (markers) indicating changes in the optical anisotropy of dehydrated films of peritoneal fluid networks.
- Clinical Validation: We clinically validated the developed methodology to facilitate early (pre-clinical) differential diagnosis of severe and prevalent pathologies, particularly endometriosis. By utilizing our approach, we aim to provide accurate and efficient diagnostic tools for detecting this condition.

3. Research Methodology

The research methodology comprises a series of sequential and complementary analytical steps. At the initial stage, the aim is to analytically determine and physically justify a set of diagnostically relevant relationships between the magnitude of the CDC (polarization-correlation parameter) and the optical anisotropy of polycrystalline structures in dehydrated films of peritoneal fluid. To achieve this, a Jones matrix description of the optical anisotropy of the polycrystalline structure in dehydrated peritoneal fluid films is proposed.

Based on the derived analytical relationships, an experimental measurement technique for obtaining spatial distributions of the CDC magnitude (polarization-correlation maps) is developed using a conventional imaging Stokes polarimeter setup.

For a representative selection of measured polarization-correlation maps, statistical, correlation, and fractal parameters are calculated. By analyzing these parameters, the most sensitive markers for changes in the polycrystalline structure of dehydrated peritoneal fluid films are identified.

4. Model Views

The analysis of the phase structure of the laser radiation field converted by blood plasma is based on the following model [1 - 15]:

- blood serum is considered as a two-component isotropic-anisotropic structure;
- the optical-anisotropic component is a fraction consisting of optically uniaxial birefringent crystals of the amino acids' albumin and globulin.
- phase properties of such biological crystals are characterized by the Jones matrix

$$\{Q\} = \begin{bmatrix} q_{11} & q_{12} \\ q_{21} & q_{22} \end{bmatrix}, \tag{1}$$

where

$$q_{ik}(r,\gamma,\varepsilon) = \begin{cases} q_{11} = cos^2\,\gamma\,(r) + sin^2\,\gamma\,(r)\,exp\big(-i\varepsilon(r)\big); \\ q_{12} = q_{21} = cos\,\gamma\,(r)\,sin\,\gamma\,(r)\big(1 - exp\big(-i\varepsilon(r)\big)\big); \\ q_{22} = sin^2\,\gamma\,(r) + cos^2\,\gamma\,(r)\,exp\big(-i\varepsilon(r)\big). \end{cases} \tag{2}$$

Here γ – optical axis direction; $\varepsilon = {}^{2\pi}/_{\lambda}\,\Delta nz$ – phase shift between orthogonal amplitude components; λ – wavelength; z– geometric path; Δn - birefringence index.

The correlation "two-point" technique for studying the polycrystalline structure of dehydrated serum films uses the following algorithm - the complex degree of coherence (CDC)

$$K_{out}(r_1,r_2) = Q^{*}(r_1) \cdot K_{in}(r_1,r_2) \cdot Q(r_2). \tag{3}$$

Here $K(r_1,r_2)$ – amplitude matrix operator

$$K(r_1,r_2) = \begin{bmatrix} U_x^*(r_1)U_x(r_2) & U_x^*(r_1)U_y(r_2) \\ U_y^*(r_1)E_x(r_2) & U_y^*(r_1)E_y(r_2) \end{bmatrix}, \tag{4}$$

where $K^{*}(r_1,r_2)$ − Hermitian conjugate matrix to $K(r_1,r_2)$; Tr - matrix spur.

Let us apply this algorithm to the analysis of the conversion of optical radiation by a birefringent layer.

$$K_{out}(r_1,r_2) = Q^{*}(r_1) \cdot K_{in}(r_1,r_2) \cdot Q(r_2). \tag{5}$$

Here $Q(r_1)$ and $Q(r_2)$ − the Jones matrix of a biological crystal at points r_1 and r_2; $K_{in}(x_1,x_2)$ – amplitude matrix of the probing beam

$$K_{in}(r_1,r_2) = \begin{bmatrix} U_x^*(r_1)E_x(r_2) & U_x^*(r_1)E_y(r_2) \\ U_y^*(r_1)E_x(r_2) & U_y^*(r_1)E_y(r_2) \end{bmatrix}. \tag{6}$$

Taking into account (1) – (6) expressions $\mu(r_1,r_2)$ (1) − (6), the expression takes the following form

$$\mu(r_1, r_2) = \sqrt{\frac{1}{(a+ib)(cos^2\,\Delta\gamma_{12}+sin^2\,\Delta\gamma_{12}\,exp(-i\cdot 2\Delta\varepsilon_{12}))}}. \quad (7)$$

Here $\Delta\gamma_{12} = \gamma(r_1) - \gamma(r_2)$, $\Delta\varepsilon_{12} = \varepsilon(r_1) - \varepsilon(r_2)$, $a + ib$ – proportionality factor.

In the future we will restrict ourselves to taking into account the CDC module

$$|\mu(r_1, r_2)| = 0{,}5(1 + cos\,2\,\Delta\varepsilon_{12})^{-1}. \quad (8)$$

Thus, to determine the magnitude of the CDC modulus, it is necessary to obtained data of phase ($\varepsilon(r_1) - \varepsilon(r_2)$) and amplitude modulation ($U_x(r_1), U_y(r_1)$ and $U_x(r_2), U_y(r_2)$) at points with coordinates r_1, r_2.

To this end, the following algorithmic scheme is used - the dehydrated serum film is placed in the optical arrangement of phase imaging - phase-shift polarizers ($\{F_1\}, \{F_2\}$) and linear polarizers ($\{L_1\}, \{L_2\}$), the transmission planes of which form angles with the directions of the axes of the highest velocity angles +45° and - 45°.

Algorithmically, the phase imaging scenario describes the equation

$$U(r) = 0{,}25\{L_2\}\{F_2\}\{Q(r)\}\{F_1\}\{L_1\}U_0. \quad (9)$$

Here

$$\begin{cases} U_0 = \begin{pmatrix} U_{0x} \\ U_{0y}\,exp(-i\varepsilon_0) \end{pmatrix}, \quad U(r) = \begin{pmatrix} U(r) \\ U_y(r)\,exp\big(-i\varepsilon(r)\big) \end{pmatrix}, \\ \{L_1\} = \begin{Vmatrix} 1 & 1 \\ 1 & 1 \end{Vmatrix}, \quad \{L_2\} = \begin{Vmatrix} 1 & -1 \\ -1 & 1 \end{Vmatrix}, \quad \{F_1\} = \begin{Vmatrix} 1 & 0 \\ 0 & i \end{Vmatrix}, \quad \{F_2\} = \begin{Vmatrix} i & 0 \\ 0 & 1 \end{Vmatrix}. \end{cases} \quad (10)$$

The algorithm (10) takes a simpler form in the case of a plane-polarized ($U_0 = \begin{pmatrix} 1 \\ 1 \end{pmatrix}$) illuminating an optically anisotropic layer

$$U(r) = 0.25 \begin{Vmatrix} 1 & -1 \\ -1 & 1 \end{Vmatrix} \begin{Vmatrix} i & 0 \\ 0 & 1 \end{Vmatrix} \times$$
$$\begin{Vmatrix} cos^2\,\gamma\,(r) + sin^2\,\gamma\,(r)\,exp[-i\varepsilon(r)] & cos\,\gamma\,(r)\,sin\,\gamma\,(r)\{1 - exp[-i\varepsilon(r)]\} \\ cos\,\gamma\,(r)\gamma(r)\{1 - exp[-i\varepsilon(r)]\} & sin^2\,\gamma\,(r) + cos^2\,\gamma\,(r)\,exp[-i\varepsilon(r)] \end{Vmatrix} \times\times \begin{Vmatrix} 1 & 0 \\ 0 & i \end{Vmatrix} \begin{Vmatrix} 1 & 1 \\ 1 & 1 \end{Vmatrix} \begin{pmatrix} 1 \\ 1 \end{pmatrix}. \quad (11)$$

The final expression (11) turns out to be the following working ratio for experimental work

$$I_\varepsilon(r) = U(r)U(r)^* = I_0\,sin^2\left[\varepsilon(r)/2\right]. \quad (12)$$

Here $I_0 \equiv 1$ – intensity of the laser beam probing a sample of dehydrated blood serum.

The result is a phase reconstruction algorithm

$$\varepsilon(r) = 2\,arcsin\sqrt{I_\varepsilon(r)}. \quad (13)$$

Based on relations (9) – (13), we obtain an expression for the algorithm for determining the CDC module of the object field of a dehydrated serum film at points r_1 and r_2

$$|\mu(r_1, r_2)| = 0{,}5\left(1 + cos\,2\left(arccos\sqrt{I(r_1)} - arccos\sqrt{I(r_2)}\right)\right)^{-1}. \quad (14)$$

The set of analytical relationships obtained, which describes the interconnections between the parameters of optical anisotropy of the polycrystalline film (equations (1), (2)), and the CDC module (equations (7), (8)), forms the foundation for the development of the experimental methodology (equations (12)-(14)) for measuring polarization-correlation maps and the physical analysis of the acquired data.

5. Method of Experimental Measurement of Polarization-Correlation Parameter

Optical scheme of polarization correlometry of the object field of dehydrated serum film at points r_1 and r_2 is shown on fig. 1 [3 - 6].

The CCD camera 10 measured a discrete two-dimensional $(m \times n)$ intensity $I_\varepsilon(m \times n)$ distribution. Further, according to (14), the coordinate distributions $\varepsilon(m \times n)$ were calculated, which were scanned with a step $\Delta r = 1pix$ along the rows $\begin{pmatrix} r_{11} & r_{11}+\Delta r & \dots & r_{1m} \\ \downarrow & & & \downarrow \\ \rightarrow & \rightarrow & \rightarrow & \rightarrow \\ \downarrow & & & \downarrow \\ r_{n1} & r_{n1}+\Delta r & \dots & r_{nm} \end{pmatrix}$ of a two-dimensional array $\varepsilon \begin{pmatrix} r_{11},\dots r_{1m} \\ \dots\dots\dots \\ r_{n1},\dots r_{nm} \end{pmatrix}$.

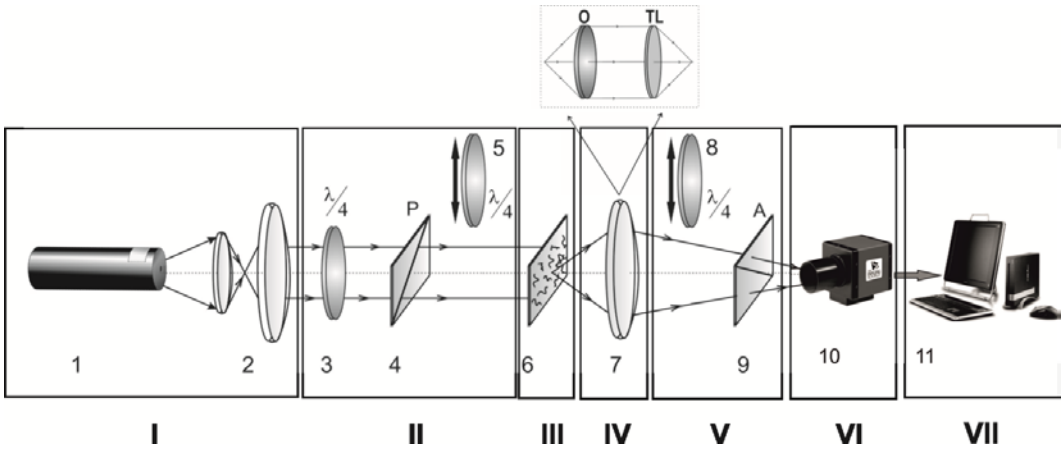

Fig. 1. Polarization correlometer: 1 - HeNe laser; 2 - optical collimator;3, 5, 8 - phase-shifting elements; 4, 9 - linear polarizer and analyzer; 6 - dehydrated serum film; 7 - polarizing micro-lens (magnification x4); 10 - digital CCD camera; 11 - computer data processing unit.

For each pair of points $(r_{ik}, r_{ik}+\Delta r)$ of the polarization-filtered object field of dehydrated serum film, based on relation (15), the value of the CDC modulus $\mu(r_{ik}, r_{ik}+\Delta r)$ was determined

As a result, a coordinate distribution $\mu\begin{pmatrix} (r_{11}; r_{11}+\Delta r) & \dots & (r_{1m-1}, r_{1m-1}+\Delta r) \\ \dots & \dots & \dots \\ (r_{n1}, r_{n1}+\Delta r) & \dots & (r_{nm-1}, r_{nm-1}+\Delta r) \end{pmatrix}$ was obtained, which will be referred to as the correlation-phase map (CPM) of the a sample of dehydrated serum film from a microscopic image.

6. Analytical Approaches to Polarization-Correlation Data Processing

We applied three methods for analytical treatment of two-dimensional arrays $\mu(1 \div m; 1 \div n)$ [20 - 28].

Statistical approach:

$$R_1^\mu = \frac{1}{M}\sum_{i=1}^{M}|\mu_i|,\ R_2^\mu = \sqrt{\frac{1}{M}\sum_{i=1}^{M}\mu_i^2},\ R_3^\mu = \frac{1}{\left(R_2^\mu\right)^3}\frac{1}{M}\sum_{i=1}^{M}\mu_i^3,\ R_4^\mu = \frac{1}{\left(R_2^\mu\right)^2}\frac{1}{M}\sum_{i=1}^{M}\mu_i^4. \quad (15)$$

Here $R_{j=1,2,3,4}^\mu$ – central statistical moments that characterize the mean, variance, skewness and kurtosis of the distribution μ(1÷m;1÷n), M - digital camera pixel count.

Correlation approach:

$$A_{i=1\div n}^\mu(\Delta m) = \lim_{m\to 0}\frac{1}{m}\int_1^m [\mu(m)][\mu(m-\Delta m)]dm. \quad (16)$$

Here $A_{i=1\div n}^\mu(\Delta m)$ – autocorrelation function, $\Delta m = 1pix$.

The final average over all lines of the digital polarization-correlation map of the serum film image is the following expression

$$A^\mu(\Delta m) = \frac{\sum_{i=1}^{n} A_i^\mu(\Delta m)}{n}. \quad (17)$$

To quantify the autocorrelation dependences $A^\mu(\Delta m)$, we chose:

- "correlation area" S^μ

$$S^\mu = \int_1^m A^\mu(\Delta m)dm; \quad (18)$$

- "correlation moment" T_4^{μ} which determines the kurtosis of the Gram-Charlier expansion

$$T = \frac{\sum_{i=1}^{M}\left(A(\Delta m)\right)_i^4}{\left(\sum_{i=1}^{M}\left(A(\Delta m)\right)_i^2\right)^2}; \quad (19)$$

Fractal approach: The fractal analysis of distributions $\mu(m \times n)$ was based on the calculation of the logarithmic dependences $log\, J\,(\mu) - log\, d^{-1}$ of the power spectra $J(\mu)$

$$J(\mu) = \int_{-\infty}^{+\infty} \mu\, cos\, 2\,\pi\nu d\nu, \quad (20)$$

where $\nu = z$ is the spatial frequencies of the of the objective field of a blood serum sample.

For the dependences $log\, J\,(\mu) - log\, d^{-1}$ the slope angle η of the approximating curves V(η) was determined and the fractal dimensions were calculated

$$F^{\mu} = 3 - tg\eta. \quad (21)$$

Classification of coordinate distributions $\mu(m \times n)$ was carried out according to the following criteria:

- $\mu(m \times n)$ – fractal or self - similar in the presence of a constant angle $\eta = const$ of inclination within 2 - 3 decades of size variations d ;
- $\mu(m \times n)$ – multifractal in the presence of several angles of inclination $V(\eta)$;
- $\mu(m \times n)$ – random in the absence of stable angles of inclination $V(\eta)$ in the entire range of resizing d.

All distributions $log\, J\,(\mu) - log\, d^{-1}$ were characterized by dispersion

$$D^{\mu} = \sqrt{\frac{1}{N}\sum_{i=1}^{N}[log\, J\,(\mu) - log\, d^{-1}]_i^2}. \quad (22)$$

7. Information Analysis

The information analysis of the results of polarization-correlation mapping utilizes a set of operational characteristics of evidence-based medicine [28]. Sensitivity (Se) is the proportion of true positive results (A) of a diagnostic method among all samples from the experimental group 2 (N).

$$Se = \frac{A}{N}100\%. \quad (23)$$

- Specificity (Sp) is the proportion of true negative results (B) of the method among all samples from the control group 1 (H).

$$Sp = \frac{B}{H}100\%. \quad (24)$$

- Accuracy (Ac) is the proportion of correct results (A+B) of the test among all samples (N+H).

$$Ac = \frac{A+B}{N+H}100\%. \quad (25)$$

If N+H, then Ac is called balanced accuracy.

8. Diagnostic efficiency of CDMP and CDC Methods

Two groups (Fig. 2) of optically thin (attenuation coefficient $\tau \leq 0.01$, geometric thickness $\approx 7\mu m \div 10\mu m$) dehydrated serum films were used as study objects. Control group 1 (39 samples) - conditionally healthy patients; study group 2 (37 samples) - patients with histologically confirmed extragenital endometriosis.

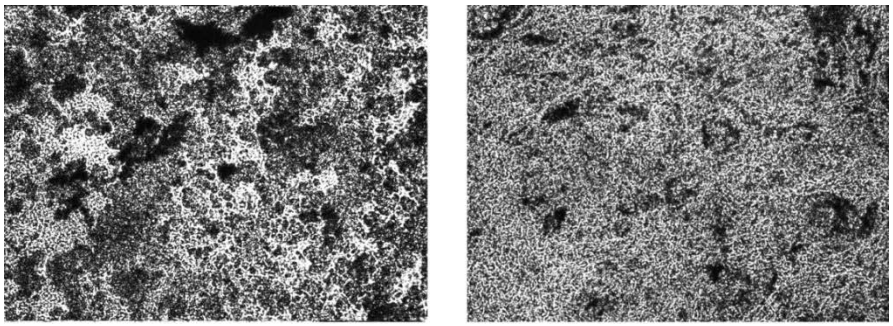

(a) (b)

Fig. 2. Polarization-visualized in crossed axes polarizer 4 and analyzer 9 microscopic images of dehydrated serum films.

On fig. 3 shows a map of the $V(m \times n)$; histograms $G(V)$: autocorrelation functions $A^V(\Delta m)$ and logarithmic dependences $log\, J^V - log\, d^{-1}$ of object images of dehydrated serum films of patients from control group 1 ((a)-(d)) and a patient with extragenital endometriosis ((e)-(h)).

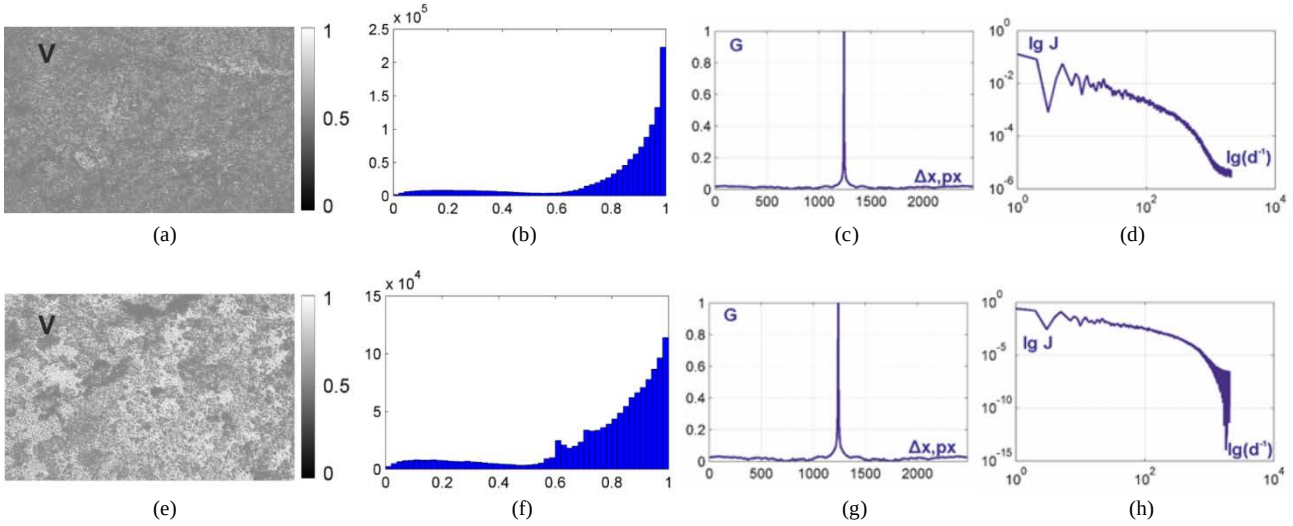

(a) (b) (c) (d)

(e) (f) (g) (h)

Fig. 3. Maps and histograms (b), (f), autocorrelation functions (c), (g) and fractal (d), (h) characteristics of CDMP (a), (e) of dehydrated serum films

Determined:

- The $G(V)$ dependences are asymmetric and possess a pronounced extremum ($V = 1$). This peculiarity can be related to the insignificant level of birefringence ($\varepsilon \approx 0.075rad \div 0.125rad$, $q_{11,22} \to 1$, $q_{12,21} \to 0$) of dehydrated serum films. The result is a high level of polarization homogeneity of such an object field.
- The correlation dependencies $A^V(\Delta m)$ of the aggregate map $V(m \times n)$decrease smoothly and monotonically (fragments (c), (g)), which also indicates the polarization homogeneity of the object field of dehydrated serum films of patients of both groups.
- The nearly monofractal structure of the $V(m \times n)$ cross-correlation maps - $log\, J^V - log\, d^{-1}$ have one stable slope angle (fragments (d), (h)).

Quantitative results of statistical, correlation and fractal analysis of CDMP maps of object fields of dehydrated serum films samples are summarized in Table 1.

Table 1. Results of statistical, correlation and fractal analysis of CDMP objective field maps of dehydrated serum film samples

Parameters	R_1^V	R_2^V	R_3^V	R_4^V	S^V	T^V	F^V	D^V
Normal (39 samples)	0.973 ± 0.042	0.057 ± 0.0027	0.083 ± 0.0039	0.77 ± 0.037	0.264 ± 0.014	0.215 ± 0.0312	2.33 ± 0.021	0.185 ± 0.011
External genital endometriosis (37 samples)	0.926 ± 0.051	0.06 ± 0.008	0.12 ± 0.007	0.62 ± 0.035	0.246 ± 0.015	0.217 ± 0.016	2.42 ± 0.014	0.21 ± 0.022

The results obtained within both sample groups showed insufficient sensitivity and diagnostic ambiguity of the CDMP method - the distribution of all objective parameters "overlap". As a consequence, the differences between the averaged values of the objective parameters do not exceed 5%-15%.

Fig. 4 illustrates the results of a study of the structure of the objective fields of dehydrated serum films using another method - the CDC method for measuring the objective fields of dehydrated serum films of patients from both groups.

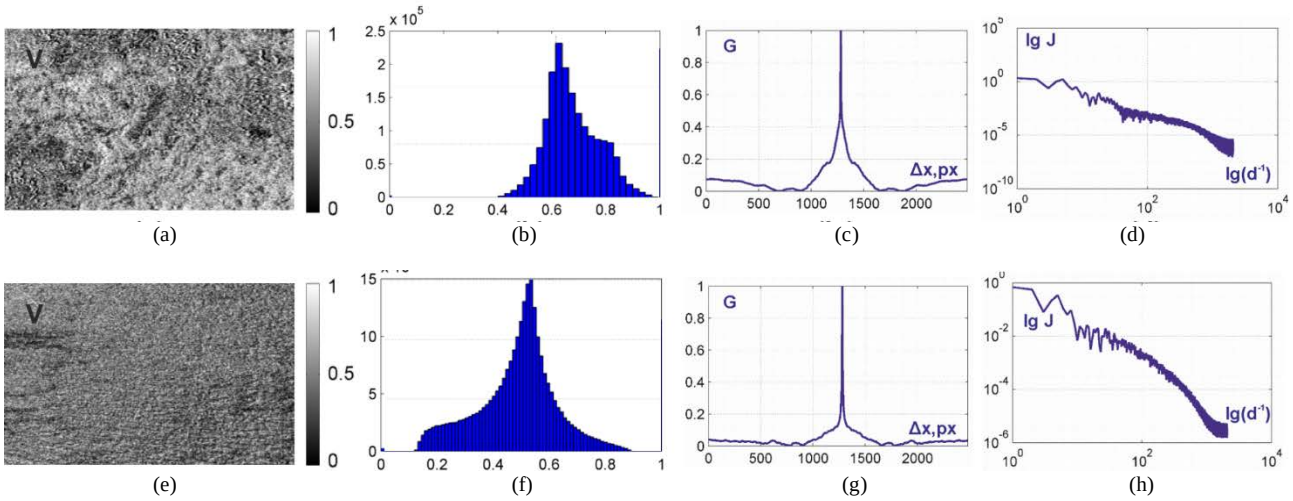

Fig. 4. Maps and histograms (b), (f), autocorrelation functions (c), (g) and fractal (d), (h) characteristics of CDC (a), (e) of dehydrated serum films.

The results indicate a significant increase in the level of sensitivity to changes in birefringence magnitude of the CDC scanning of the object fields of dehydrated serum films. This is indicated by the significant intergroup variation in histograms, autocorrelation functions and fractal characteristics obtained by CDC detection (Fig. 4) and Table 2.

Table 2. Results of statistical, correlation and fractal analysis of CDC maps of object fields of dehydrated serum film samples

Parameters	R_1^V	R_2^V	R_3^V	R_4^V	S^V	T^V	F^V	D^V
Normal (39 samples)	0.79 ± 0.039	0.079 ± 0.009	0.049 ± 0.021	0.29 ± 0.021	0.26 ± 0.01	0.23 ± 0.032	1.89 ± 0.022	0.17 ± 0.021
External genital endometriosis (37 samples)	0.67 ± 0.038	0.13 ± 0.018	0.425 ± 0.027	1.13 ± 0.037	0.165 ± 0.012	0.86 ± 0.091	-	0.24 ± 0.033

The following differences between the objective parameters that characterize CDC maps of dehydrated serum films were found:

- statistical moments of higher orders differ by a factor of 7 - 10;
- correlation parameters differ by a factor of 1.5 to 3.98;
- fractal parameters of object fields of serum films from group 1 are transformed into a random distribution for samples of group 2.

The results of the information analysis regarding the determination of the clinical effectiveness of the proposed method of polarization-correlation mapping of peritoneal fluid films are presented in Table 3.

Table 3. Accuracy of the differential diagnosis of polarization-correlation mapping of images of dehydrated serum film samples.

Parameters	R_1^V	R_2^V	R_3^V	R_4^V	S^V	T^V	F^V	D^V
Accuracy, %	84	81	88	91	90	95	82	86

The analysis of polarization-correlation mapping data determined the following accuracy levels for the differential diagnosis of endometriosis using different markers:

- Statistical analysis - good accuracy $Ac(R_4^V) = 91\%$;
- Correlation analysis - excellent accuracy $Ac(T^V) = 95\%$;
- Fractal analysis - satisfactory accuracy $Ac(D^V) = 86\%$.

However, these are only preliminary results from the clinical evaluation of the polarization-correlation mapping method. Ahead lies extensive systematic work for the wide-scale implementation of the developed technique, considering the influence of numerous demographic, societal, social, and other factors on its reproducibility, accuracy, and clinical effectiveness.

9. Conclusions

A theory of polarization-correlation description of laser radiation conversion processes by birefringent dehydrated serum films is proposed.

Basic algorithms of two-point approach for analysis of optical anisotropy of polycrystalline serum films are found.

A method of polarization correlometry of phase-inhomogeneous object fields of dehydrated serum films was developed and experimentally tested.

The diagnostic sensitivity of the CDC method in differentiating dehydrated serum films of healthy and diseased patients with extragenital endometriosis has been demonstrated.

The proposed technique expands the functional capabilities of traditional histological examinations of endometrial tissue biopsies and enables the detection of endometriosis at early (preclinical) stages.

Acknowledgments

This work received funding from: National Research Foundation of Ukraine, Project 2020.02/0061; National Research Foundation of Ukraine, Project 2022.01/0034 and Scholarship of the Supreme Council for Young Scientists—Doctors of Sciences.

Conflict of Interest

The authors declare no competing interests.

Ethics Approval and Consent to Participate

This study was conducted in accordance with the principles of the Declaration of Helsinki, and in compliance with the International Conference on Harmonization-Good Clinical Practice and local regulatory requirements. Ethical approval was obtained from the Ethics Committee of the Bureau of Forensic Medicine of the Chernivtsi National University and the Bukovinian State Medical University (Chernivtsi, Ukraine), and written informed consent was obtained from all subjects prior to study initiation.

References

[1] Ushenko, A. G. & Pishak, V. P. Laser Polarimetry of Biological Tissues: Principles and Applications. in Handbook of Coherent Domain Optical Methods (ed. Tuchin, V. V. (Valeriĭ V.) 93–138 (Springer US, 2004). doi:10.1007/0-387-29989-0_3.

[2] Ghosh, N. Tissue polarimetry: concepts, challenges, applications, and outlook. J. Biomed. Opt. 16, 110801 (2011).

[3] Jacques, S. L. Polarized light imaging of biological tissues. in Handbook of Biomedical Optics2 (eds. Boas, D., Pitris, C. & Ramanujam, N.) 649–669 (CRC Press, 2011).

[4] Vitkin, A., Ghosh, N. & de Martino, A. Tissue Polarimetry. in Photonics: Scientific Foundations, Technology and Applications (ed. Andrews, D. L.) 239–321 (John Wiley & Sons, Ltd, 2015).

[5] Anton Sdobnov, Volodymir A. Ushenko, Liliya Trifonyuk, Oksana Bakun, Marta Garazdyuk, Irina V. Soltys, Olexander Dubolazov, Olexander G. Ushenko, Yuriy A. Ushenko, Alexander Bykov, Igor Meglinski,,Mueller-matrix imaging polarimetry elevated by wavelet decomposition and polarization-singular processing for analysis of specific cancerous tissue pathology, J. Biomed. Opt. 28(10), 102903 (2023), doi: 10.1117/1.JBO.28.10.102903

[6] Ushenko, Y. A., Boychuk, T. M., Bachynsky, V. T. & Mincer, O. P. Diagnostics of Structure and Physiological State of Birefringent Biological Tissues: Statistical, Correlation and Topological Approaches. in Handbook of Coherent-Domain Optical Methods (ed. Tuchin, V. V. (Valeriĭ V.) vols 1–2 107–148 (Springer New York, 2013).

[7] P O Angelsky, A G Ushenko, A V Dubolazov, M I Sidor, G B Bodnar, G Koval and L Trifonyuk. The singular approach for processing polarization-inhomogeneous laser images of blood plasma layers// Journal of Optics, 2013Volume 15, Number 4

[8] Vasyl P Pishak, Alexander G Ushenko, Petro Gryhoryshyn, et. al. Polarization structure of biospeckle fields in crosslinked tissues of a human organism: 1. Vector structure of skin biospeckles// Proceedings Volume 3317, International Conference on Correlation Optics; (1997) https://doi.org/10.1117/12.295715

[9] Volodimir Ushenko, Anton Sdobnov, Anna Syvokorovskaya, et.al. 3D Mueller-Matrix Diffusive Tomography of Polycrystalline Blood Films for Cancer Diagnosis//Photonics 2018, 5(4), 54.

[10] N. I. Zabolotna, S. V. Pavlov, et.al. “System of the phase tomography of optically anisotropic polycrystalline films of biological fluids” Proceedings Volume 9166, Biosensing and Nanomedicine VII; 916616 (2014)
[11] G Ushenko, A. V. Dubolazov, V. O. Balanets'ka, A. V. Karachevtsev, M. Sydor. Wavelet analysis for polarization inhomogeneous laser images of blood plasma//Proceedings Volume 8338, Tenth International Conference on Correlation Optics; 83381H (2011)
[12] Ushenko, V.A., Hogan, B.T., Dubolazov, A., Grechina, A.V., Boronikhina, T.V., Gorsky, M., Ushenko, A.G., Ushenko, Y.O., Bykov, A., Meglinski, I.Embossed topographic depolarisation maps of biological tissues with different morphological structures, (2021) Scientific Reports, 11 (1), № 3871.
[13] Peyvasteh, M., Tryfonyuk, L., Ushenko, V., Syvokorovskaya, A.-V., Dubolazov, A., Vanchulyak, O., Ushenko, A., Ushenko, Y., Gorsky, M., Sidor, M., Tomka, Y., Soltys, I., Bykov, A., Meglinski, I., 3D Mueller-matrix-based azimuthal invariant tomography of polycrystalline structure within benign and malignant soft-tissue tumours, (2020) Laser Physics Letters, 17 (11), 115606.
[14] Trifonyuk, L., Strashkevich, A., Pavlyukovich, N., Pavlyukovich, A., Tomka, Yu., Zhitaryuk, V., Tkachuk, V.I. Polarization interference mapping of microscopic images of protein fluorofores in the differential diagnosis of benign and malignant prostate tumours (2021) Proceedings of SPIE - The International Society for Optical Engineering, 12126, 1212628.
[15] Trifonyuk, L., Strashkevich, A., Kozlov, S., Davidenko, I., Poliansky, I., Pavlyukovich, N., Pavlyukovich, A., Tomka, Yu., Fesiv, I.V., Ushenko, Yu.A., Talakh, M., Gorodenskiy, P.A., Gantyuk, V.K. Digital microscopic mapping of laser induced polarization ellipticity maps in differential diagnostics of preparations of benign and malignant prostate tumours (2021) Proceedings of SPIE - The International Society for Optical Engineering, 12126, 1212627.
[16] Kvasniuk, D., Trifonyuk, L., Strashkevich, A., Kozan, N., Ushenko, V., Dunaiev, O., Kryvetskyi, V., Oliinyk, I., Kurek, E.I., Tkachuk, V.I. Detection of pathological changes in the architectonics of polycrystalline blood films using laser-induced polarization interferometry (2021) Proceedings of SPIE - The International Society for Optical Engineering, 12126, 1212629.
[17] Beam coherence polarization matrix / F. Gori, M. Santarsiero, S. Vicalvi, R. Borghi, G. Guattari // Pure Appl. Opt. – 1998. – Vol. 7. – P. 941-951.
[18] J. Tervo, T. Setala, A. Friberg, “Two-point Stokes parameters: interpretation and properties," Optics Letters 34(20), 3074 - 3076 (2009).
[19] Ushenko Yu. A. Spatial-frequency Fourier polarimetry of the complex degree of mutual anisotropy of linear and circular birefringence in the diagnostics of oncological changes in morphological structure of biological tissues / Yu. A. Ushenko, M. P. Gorskii, A. V. Dubolazov, A. V. Motrich, V. A. Ushenko, M. I. Sidor // Quantum Electron, 2012, Volume 42(8).
[20] Ushenko V. A. Complex degree of mutual anisotropy of linear birefringence and optical activity of biological tissues in diagnostics of prostate cancer / V. A. Ushenko, M. P. Gorsky. // Optics and Spectroscopy, August 2013, Volume 115, Issue 2, pp 290-297.
[21] Yu. A. Ushenko, V. T. Bachynsky, O. Ya. Vanchulyak, A. V. Dubolazov, M. S. Garazdyuk, and V. A. Ushenko, “Jones-matrix mapping of complex degree of mutual anisotropy of birefringent protein networks during the differentiation of myocardium necrotic changes,” Appl. Opt. 55, B113-B119 (2016).
[22] Alexander Ushenko, Anton Sdobnov, Alexander Dubolazov, Marta Gritsuk, Yurii Ushenko, Alexander Bykov, Igor Meglinski, “Stokes-Correlometry Analysis of Biological Tissues with Polycrystalline Structure,” IEEE Journal of Selected Topics in Quantum Electronics 25, 7101612 (2018).
[23] Motahareh Peyvasteh, Alexander Dubolazov, Alexey Popov, Alexander Ushenko, Yuriy Ushenko and Igor Meglinski, “Two-point Stokes vector diagnostic approach for characterization of optically anisotropic biological tissues,” J. Phys. D: Appl. Phys. 53, 395401 (2020).
[24] Ushenko, V.A., Hogan, B.T., Dubolazov, A. et al. 3D Mueller matrix mapping of layered distributions of depolarisation degree for analysis of prostate adenoma and carcinoma diffuse tissues. Sci Rep 11, 5162 (2021). https://doi.org/10.1038/s41598-021-83986-4
[25] Zhengbing Hu, Ihor Tereikovskyi, Denys Chernyshev, Liudmyla Tereikovska, Oleh Tereikovskyi, Dong Wang, " Procedure for Processing Biometric Parameters Based on Wavelet Transformations ", International Journal of Modern Education and Computer Science, Vol.13, No.2, pp. 11-22, 2021.
[26] Yuriy O. Ushenko, Yuriy Ya. Tomka, Igor Z. Misevitch, Vadim V. Istratyy, and Olga I. Telenga "Complex degree of mutual anisotropy of biological liquid crystals nets," Optical Engineering 50(3), 039001 (1 March 2011). https://doi.org/10.1117/1.3558850
[27] Zhengbing Hu, Sergiy Gnatyuk, Tetiana Okhrimenko, Sakhybay Tynymbayev, Maksim Iavich, "High-Speed and Secure PRNG for Cryptographic Applications", International Journal of Computer Network and Information Security, Vol.12, No.3, pp.1-10, 2020.
[28] S. P. Robinson, Principles of forensic medicine, Cambridge University Press (1996).

Authors’ Profiles

Yuriy Ushenko, Was born on December 23, 1980 in Chishinau, Moldova. M.Sc. in Telecommunications (2003). PhD in Optics and Laser Physics (2006). D.Sc. in Optics and Laser Physics, Taras Shevchenko National University of Kyiv (2015). Current position – Professor, Head of Computer Science Department, Chernivtsi National University, Ukraine. Research Interests: Data Mining and Analysis, Computer Vision and Pattern Recognition, Optics & Photonics, Biophysics.

Ivan Gordey, Post-graduate student at the Computer Science Department of the Institute of Physical and Technical and Computer Sciences at the Yuri Fedkovich Chernivtsi National University. His research interests include digital processing of medical images using computer algorithms of statistical, correlation and fractal analysis.

Yuriy Tomka was born on Septemer 13, 1983 in Chernivtsi, Ukraine. M.Sc. in Laser and optoelectronic technology (2005). PhD in Optics and Laser Physics (2008). Current position – Associate Professor, Computer Science Department, Chernivtsi National University, Ukraine. Research Interests: Software engineering, Software architecture, Biomedical Imaging, Computer Vision, Optics & Photonics, Biophysics, Laser Polarimetry.

Iryna Soltys, In 2010 she graduated from the Chernivtsi National University. She received her BS and MS degrees in optics from the Chernivtsi National University in 2009 and 2010, respectively, and his PhD degree in optics, laser physics from the Chernivtsi National University in 2013. She is an Associate Professor at the Chernivtsi National University. She is the author of more than 60 journal papers and has written five book chapters. She current research interests include laser polarimetry, holography etc.

Oksana Bakun, Obstetrics and Gynecology Department, Bukovinian State Medical University,Teatralna Sq.,2, Ukraine, Chernivtsi,58000 Ukraine Current Position: Doctorate, PhD, Candidate of Medical Sciences.

Zhengbing Hu, Prof., Deputy Director, International Center of Informatics and Computer Science, Faculty of Applied Mathematics, National Technical University of Ukraine “Kyiv Polytechnic Institute”, Ukraine. Adjunct Professor, School of Computer Science, Hubei University of Technology, China. Visiting Prof., DSc Candidate in National Aviation University (Ukraine) from 2019. Major research interests: Computer Science and Technology Applications, Artificial Intelligence, Network Security, Communications, Data Processing, Cloud Computing, Education Technology.

How to cite this paper: Yuriy Ushenko, Ivan Gordey, Yuriy Tomka, Irina Soltys, Oksana Bakun, Zhengbing Hu, "Information Technology for Multiparametric Analysis of Laser Images of Biological Fluid Films in Biomedical Applications", International Journal of Image, Graphics and Signal Processing(IJIGSP), Vol.15, No.5, pp. 77-87, 2023. DOI:10.5815/ijigsp.2023.05.06